Learning Motion Categories using both Semantic and Structural Information

Shu-Fai Wong, Tae-Kyun Kim and Roberto Cipolla
Department of Engineering,
University of Cambridge,
Cambridge, CB2 1PZ, UK
{sfw26, tkk22, cipolla}@eng.cam.ac.uk

Abstract

Current approaches to motion category recognition typically focus on either full spatiotemporal volume analysis (holistic approach) or analysis of the content of spatiotemporal interest points (part-based approach). Holistic approaches tend to be more sensitive to noise e.g. geometric variations, while part-based approaches usually ignore structural dependencies between parts. This paper presents a novel generative model, which extends probabilistic latent semantic analysis (pLSA), to capture both semantic (content of parts) and structural (connection between parts) information for motion category recognition. The structural information learnt can also be used to infer the location of motion for the purpose of motion detection. We test our algorithm on challenging datasets involving human actions, facial expressions and hand gestures and show its performance is better than existing unsupervised methods in both tasks of motion localisation and recognition.

1. Introduction

With the abundance of multimedia data, there is a great demand for efficient organisation of images and videos in an unsupervised manner so that the data can be searched easily. In this paper, we will focus on the motion categorisation problem for video organisation.

Among traditional approaches to motion categorisation, computing correlation between two spatiotemporal (ST) volumes (i.e. whole video inputs) is the most straightforward method. Various correlation methods such as cross correlation between optical flow descriptors [4] and a consistency measure between ST volumes from their local intensity variations [13] have been proposed. Although this approach is easy to understand and implement and makes a good use of geometrical consistency, it cannot handle large geometric variation between intra-class samples, moving cameras and non-stationary backgrounds, and it is also computational demanding for motion localisation in large ST volumes.

Instead of performing the above holistic analysis, many researchers have adopted an alternative, part-based approach. This approach uses only several 'interesting' parts of the whole ST volume for analysis and thus avoids problems such as non-stationary backgrounds. The parts can be trajectories [16] or flow vectors [15, 5] of corners, profiles generated from silhouettes [1] and ST interest points [9, 3, 8]. Among them, ST interest points can be obtained more reliably and thus be widely adopted in motion categorisation where discriminative classifiers such as support vector machines (SVM) [12] and boosting [8], and generative models such as probabilistic latent semantic analysis (pLSA) [11] and specific graphical models [2] have been exploited. When considering a huge amount of unlabelled video, generative models, which require the least amount of human intervention, seem to be the best choice.

Currently used generative models for part-based motion analysis still have room for improvement. For instance, Boiman and Irani's work [2] is designed specifically for irregularity detection only, and Niebles et al.'s work [11] ignores structural (or geometrical) information which may be useful for motion categorisation. As shown in Figure 1, 3D (ST) interest regions generated by walking sequences geometrically distribute in a different way than those from a hand waving sequence. Adding structural information into the generative models, however, is not a trivial task and may increase time complexity dramatically. Inspired by the 2D image categorisation works of Fergus et al. [6] and Leibe et al. [10], we first extend the generative models for 2D image analysis, which uses structural information, to 3D video analysis, and then propose a novel generative model called pLSA with an implicit shape model (pLSA-ISM) which can make use of both semantic (the content of ST interest regions or *cuboids*) and structural (geometrical relationship between cuboids) information for efficient inference of motion category and location. A retraining algorithm which can improve an initial model using unsegmented data in an unsupervised manner is also proposed in this paper. Next section will describe the proposed model in details.

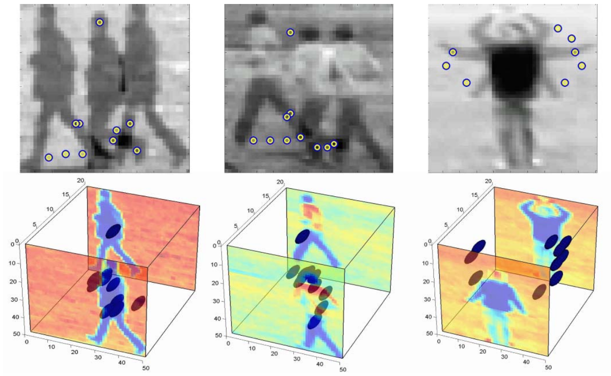

Figure 1. Top row shows superposition images of two walking sequences and a hand waving sequence. Spatiotemporal (ST) interest points (detected by method proposed in [3]) are also displayed. Bottom row shows the 3D visualisation of those ST points.

2. Approach

Before describing our approach, we first review pLSA and its variations applied in 2D object categorisation.

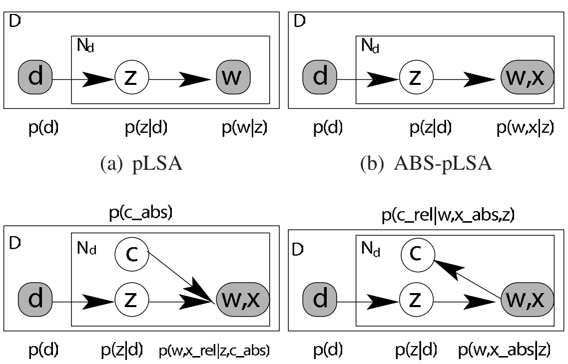

(a) pLSA (b) ABS-pLSA

(c) TSI-pLSA (d) pLSA-ISM

Figure 2. Graphical models of various pLSA described.

2.1. Classical pLSA

Classical pLSA was originally used in document analysis. Following the notation used in Sivic et al. [14] and referring to Figure 2(a), we have a set of D Documents and each of them contains a set of N_d Words. All words from the set of D documents can be vector quantitised into W word classes (code-words) which form a codebook. The corpus of documents can then be represented by a co-occurrence matrix of size $W \times D$, with entry $n(w, d)$ indicating the number of code-word w in document d. Apart from documents and words which are observable from data, we also have an unobservable variable, z, to describe Z Topics covered in documents and associated with words. The pLSA algorithm can be used to learn the associations: $P(w|z)$ (words that can be generated from a topic) and $P(z|d)$ (the topic of a document) through an Expectation-Maximisation (EM) algorithm [7] applied on the co-occurrence matrix.

The pLSA model can be applied in 2D image analysis [14] by replacing 'words' by interest *patches* and 'documents' by *images*, and in 3D motion analysis [11] by replacing 'words' by *cuboids* and 'documents' by *videos*.

2.2. Absolute position pLSA(ABS-pLSA)

In image analysis, structural information (i.e. geometric relationship between interest patches) can be used to improve the original pLSA model. Fergus et al. [6] proposed to quantitise location measurement of patches in an absolute coordinate frame to a discrete variable x_{abs} and to learn a joint density $P((w, x_{\text{abs}})|z)$ instead of $P(w|z)$ in pLSA. Referring to Figure 2(b), the new model can be trained using the standard pLSA by substituting (w, x_{abs}) into w of the original pLSA model.

2.3. Translation and Scale Invariant pLSA (TSI-pLSA)

ABS-pLSA is simple to implement, but sensitive to translation and scale changes. Thus, Fergus et al. [6] extended it to be translation and scale invariant by introducing a latent variable c_{abs} (in an absolute coordinate frame) for representing centroid locations (See Figure 2(c)). In short, relative location x_{rel} (w.r.t. centroid) is used instead of an absolute one so that the model built is translation and scale invariant. To avoid doing computational expensive inference on estimating centroid locations, Fergus et al. proposed to use a sampling scheme where centroid samples are obtained by clustering interest patches based on their likelihood $P(w|z)$ on a certain topic and their spatial locations. The term $P((w, x_{\text{rel}})|z)$ (with relative location x) can then be obtained by marginalisation, $\sum_c P((w, x_{\text{rel}})|c_{\text{abs}}, z)P(c_{\text{abs}})$ using the centroid samples.

2.4. pLSA with implicit shape model (pLSA-ISM)

Although TSI-pLSA can capture structural information while being translation and scale invariant, it cannot be used in complicated inference such as inferring the centroid location from a patch and its location (i.e. $P(c_{\text{abs}}|w, x_{\text{abs}})$ or our localisation task described later). Besides, the spatial clustering algorithm involved in estimation of centroid location can be quite sensitive to outliers especially when the number of patches detected is small (this is usually the case in ST cuboid detection). Since both ABS-pLSA and TSI-pLSA have not been applied in video analysis, their performance in this domain is unknown.

Inspired by the work of Leibe et al. [10] who proposed the use of an implicit shape model (ISM) to infer the object location in an image, we can improve TSI-pLSA by re-interpreting its graphical model. Before describing our proposed model, we briefly explain ISM first. It is a model for image analysis and it captures the association between patches and their locations by a probability distribution $P(c_{\rm rel}|(w, x_{\rm abs}))$ which represents the distribution of relative centroid locations given an observed patch. If patches belong to a single object (i.e. with the same absolute centroid location), relative locations between patches can be inferred from the distribution. Therefore, Leibe et al. named it as an implicit shape model. The distribution can be learnt offline by counting the frequency of co-occurrence of a patch $(w, x_{\rm abs})$ and its object centroid location $(c_{\rm rel})$. In recognition, the object location can be inferred by a probabilistic Hough voting scheme [10]: $P(c_{\rm abs}) = \sum_{(w,x_{\rm abs})} P(c_{\rm rel}|(w, x_{\rm abs}))P(w, x_{\rm abs})$.

We borrow the idea of the implicit shape model (on 2D inputs) to help re-interpreting the TSI-pLSA model (on 2D inputs) such that the new model can be used to learn structural information for complicated inference processes in video analysis (3D inputs). The overall idea can be illustrated by Figure 2(d) which shows the inference direction between c and (w, x) are inverted compare with that in TSI-pLSA. In mathematical terms, all presented pLSA models supporting structural information involve a term $P((w, x)|z)$ as a model parameter, and different models have their own way to interpret this parameter while their learning algorithms are basically the same. In ABS-pLSA, the parameter is set as $P((w, x_{\rm abs})|z)$ while in TSI-pLSA, it is set as $P((w, x_{\rm rel})|z)$ which is computed from $\sum_c P((w, x_{\rm rel})|z, c_{\rm abs})P(c_{\rm abs})$ corresponding to an arrow direction from c to (w, x). In our proposed model, we interpret the term in a way that inverts the arrow direction:

$$P((w, x_{\rm rel})|z) = \sum_c P(c_{\rm rel}|(w, x_{\rm abs}), z)P((w, x_{\rm abs})|z). \tag{1}$$

From this interpretation, we can obtain a term, $P(c_{\rm rel}|(w, x_{\rm abs}), z)$, which indicates the probability of having a certain centroid location $(c_{\rm rel})$ given a certain patch observation $(w, x_{\rm abs})$ and under a certain topic z. This term can be thought as an implicit shape model (i.e. $P(c_{\rm rel}|(w, x_{\rm abs}))$ in [10]) giving the association between patches and their locations (linked by a relative centroid).

As in [10], instead of computing and storing $P(c_{\rm rel}|(w, x_{\rm abs}), z)$, we operate on $P(c_{\rm rel}|w, z)$ or $P(x_{\rm rel}|w, z)$ (considering a centroid (m_x, m_y) from a patch location implies the patch located at $(-m_x, -m_y)$ w.r.t. centroid) so that $x_{\rm abs}$ is used only when we need to infer $c_{\rm abs}$ in the localisation step (see Section 2.4.2). It follows that we can convert the pLSA parameter $P((w, x_{\rm rel})|z)$ to the implicit shape model parameter $P(x_{\rm rel}|w, z)$ by:

$$P(x_{\rm rel}|w, z) = \frac{P((w, x_{\rm rel})|z)}{\sum_{x_{\rm rel}} P((w, x_{\rm rel})|z)}. \tag{2}$$

2.4.1 Training algorithm

As we have seen before, different pLSA models supporting structural information have their own way to interpret its model parameter but can share the same learning algorithm. We can make use of the EM algorithm to infer the pLSA model parameter $P((w, x_{\rm rel})|z)$ and then to obtain the implicit shape model $P(x_{\rm rel}|w, z)$ using Equation 2. The training algorithm is summarised in Algorithm 1.

Algorithm 1 Training algorithm for pLSA-ISM

if $c_{\rm abs}$ is known **then**
- Quantitise absolute locations to relative locations $x_{\rm rel}$.
- Combine $x_{\rm rel}$ and w into a single discrete variable $(w, x_{\rm rel})$ and run standard pLSA model on this variable (i.e. run ABS-pLSA) to obtain $P((w, x_{\rm rel})|z)$.

else
- Obtain a set of candidate centroid locations and scales, $c_{\rm abs}$ as in [6] (see Section 2.3).
- Obtain the pLSA parameter, $P((w, x_{\rm rel})|z)$ from TSI-pLSA.

end if
- Obtain the implicit shape model parameter $P(x_{\rm rel}|w, z)$ and a parameter $P(z|w)$ from the pLSA parameter, $P((w, x_{\rm rel})|z)$.

2.4.2 Localisation and Recognition algorithms

The implicit shape model parameter $P(x_{\rm rel}|w, z)$ and the pLSA model parameter $P((w, x_{\rm rel})|z)$ learnt from the training process are used in the localisation task and the recognition task respectively. In the localisation task, the probabilistic Hough voting scheme proposed in [10] is used to infer centroid locations (refer to Algorithm 2).

Algorithm 2 Localisation algorithm of pLSA-ISM

- Obtain an occurrence table for $P(c_{\rm rel}|w)$ (computed from $\sum_z P(x_{\rm rel}|w, z)P(z|w)$).
- Initialise an occurrence map for $P(c_{\rm abs})$.

for $i = 1$ to noOfDetection **do**
- Obtain $(w, x_{\rm abs})_i$ from each cuboid.
- Infer a relative centroid location $c_{\rm rel}$ from $P(c_{\rm rel}|w)$ and w.
- Compute the absolute centroid location $c_{\rm abs}$ from $c_{\rm rel}$ and $x_{\rm abs}$.
- Increase the $P(c_{\rm abs})$ by $P(c_{\rm rel}|w)$ computed above.

end for
- Obtain candidate centroid locations from $P(c_{\rm abs})$.

In the recognition task, an intermediate variable $(w, x_{\rm rel})$ can be obtained from a given test input $d_{\rm test}$ and the candidate centroid locations computed from Algorithm 2. The ABS-pLSA algorithm can then be exploited to infer $P(z|d_{test})$ to give a recognition result from the variable.

2.4.3 Retraining algorithm

Assuming we have an initial pLSA-ISM model, we can retrain it using unsegmented data (i.e. with unknown c_{abs}) in an unsupervised manner using Algorithm 3.

Algorithm 3 Retraining algorithm of pLSA-ISM

- Obtain a candidate centroid location using pLSA-ISM localisation algorithm if unsegmented data is given.
- Quantitise absolute locations to discrete and relative locations x_{rel}.
- Combine x_{rel} and w into a single discrete variable (w, x_{rel}).
- Concatenate new data to old data.
- Run standard pLSA model to give an updated $P((w, x_{\text{rel}})|z)$.
- Obtain an updated implicit shape model parameter $P(x_{\text{rel}}|w, z)$ from the updated pLSA parameter, $P((w, x_{\text{rel}})|z)$.

2.5. Implementation details

Similar to most part-based algorithms for image and video analysis, we first convert inputs (i.e. videos in our case) into parts (i.e. ST cuboids). This conversion is done by ST interest point detection on videos which have been transformed into greyscale format and resized to a moderate size ($x : 50 \times y : 50 \times t : 20$ was used). Among various ST point detectors such as [9, 3], Dollár et al. [3] detector was chosen to achieve the best recognition result. The spatial and temporal scale were set to 2 and 4 respectively and each cuboid is encoded using spatiotemporal gradient as recommended in Dollár et al. [3].

Eventually, for each input video d, we obtain N_d cuboids. K-means clustering is done on all cuboids from videos in a training set based on their appearance w and location x and then semantic and structural codebooks are formed from the cluster centres. Vector quantitisation is then performed on all cuboids so that each of them is quantitised into one of the $(W \times X)$ code-words. Co-occurrence matrix of size $(W \times X) \times D$ (where D is the number of videos for training) is then formed by concatenating cuboid histograms (each with size $(W \times X) \times 1$) of videos in the training set. The co-occurrence matrix can be served as an input of the pLSA algorithms (with the number of iteration set to 100) described in the previous section and pLSA model parameters, $P(z|d)$ and $P((w, x)|z)$, can be learnt for testing. In our experiments, the number of topic, Z, was set slightly larger than the number of motion category involved (around 10). The motion class, t, can be inferred from the topic reported using $P(t|z)$ which can be estimated by counting the occurrence of topics and motion classes in the training set.

3. Experiments

3.1. Datasets

We conducted experiments in three different domains, namely human activity, facial expression and hand gesture. The human activity dataset (KTH dataset [1]) was introduced by Schuldt et al. [12], the facial expression dataset was collected by Dollár et al. [3] and the hand gesture dataset was captured by us. Table 1 summarises the details of them and Figure 3 shows samples from them. We performed leave-one-out cross-validation to evaluate our algorithm so that videos from a certain subject under a certain condition were used in testing and the remaining were used in training. The result is reported as the average of all possible runs.

Dataset	KTH (segmented)	Facial Expression	Gesture
No. of classes	6	6	9
No. of subjects	25	2	2
No. of capturing conditions	4	2	5
No. of trials per subject	1	8	10
Total No. of samples	593	192	900
No. of samples used in codebook formation	240	48	90

Table 1. Details of the dataset used in our experiments.

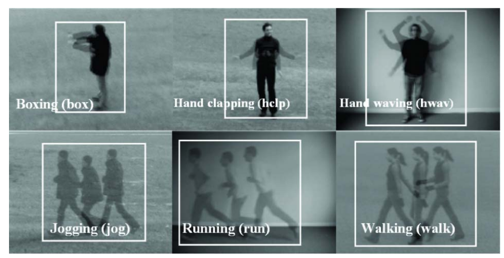

(a) KTH

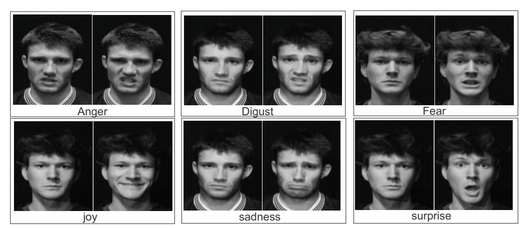

(b) Facial Expression

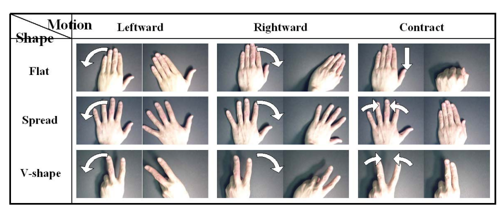

(c) Gesture

Figure 3. Sample images in the three datasets used.

[1] The original KTH dataset was processed such that actions presented in it are aligned and there is one iteration of action per sample. We refer the original dataset as unsegmented KTH and the processed one as segmented KTH.

3.2. Algorithms for Comparison

Since the experimental setting (e.g. the size of training sets) of previous studies such as [12, 11] are not the same as ours and the results cannot be compared directly, thus, we ran our implementations of their methods using a unified setting. The setting used was obtained empirically such that the recognition rate of standard pLSA is maximised. The code was written in Matlab running in a P4 1GB memory computer. Table 2 and 3 summarise the algorithms and the setting used respectively. The recognition algorithm using Support Vector Machines (SVM) was implemented based on Schuldt et al. work [12], with a replacement of its local kernel by a radial kernel on histogram inputs so that both SVM and pLSA models used the same input.

Algorithm	Description
pLSA	pLSA applied on (w) histogram
ABS-pLSA	ABS-pLSA applied on (w, x_{abs}) histogram
TSI-pLSA	TSI-pLSA applied on (w, x_{rel}) histogram
pLSA-ISM	our pLSA-ISM applied on (w, x_{rel}) histogram
W-SVM	SVM applied on (w) histogram
WX-SVM	SVM applied on (w, x_{rel}) histogram

Table 2. Details of the algorithms used in our experiments.

Dataset	KTH	Facial Expression	Gesture
No. of samples for training (D)	570	144	720
No. of cuboids (N_d)	100	100	100
Size of the semantic codebook (W)	100	50	100
Size of the structural codebook (X)	15	15	10
No. of topics (Z)	20	20	20

Table 3. The pLSA setting used in our experiments.

3.3. Results

3.3.1 Recognition

Since video samples from all three datasets used are well segmented, there is only small difference in performance between ABS-pLSA, TSI-pLSA and our pLSA-ISM. Therefore, we show only experimental results on recognition obtained from pLSA, pLSA-ISM, W-SVM and WX-SVM. The results are summarised in Table 4 and the confusion matrices obtained by our method pLSA-ISM are given in Figure 4.

From experiments, we can observe that structural information plays an important role in improving recognition accuracy (note that the accuracy obtained by WX-SVM is higher than that obtained by W-SVM, and similarly pLSA-ISM works better than pLSA). It is also found that the SVMs used scored better than the pLSA algorithms. However, SVMs require labelled data as an input while the pLSA models can learn categories in an unsupervised manner.

	pLSA	W-SVM	pLSA-ISM	WX-SVM
KTH:				
- Accuracy(%)	68.53	78.21	83.92	91.6
- Training time (s)	82.20	1.84	1.4e+3	3.59
- Testing time (s)	0.25	0.17	5.48	0.25
Facial Expression:				
- Accuracy(%)	50.00	62.04	83.33	88.54
- Training time (s)	9.90	0.21	175.54	0.29
- Testing time (s)	0.62	0.08	7.98	0.12
Gesture:				
- Accuracy(%)	76.94	86.13	91.94	97.78
- Training time (s)	121.06	3.18	1.2e+3	5.39
- Testing time (s)	8.20	0.27	47.25	1.32

Table 4. Comparison between recognition results obtained from pLSA, pLSA-ISM and SVMs.

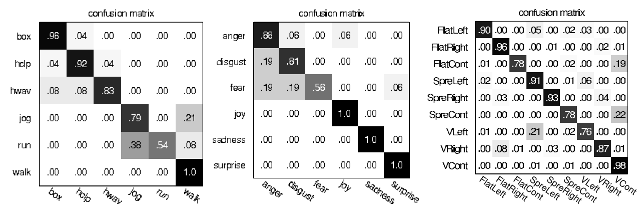

(a) KTH (b) Facial Expression (c) Gesture

Figure 4. Confusion matrices generated by applying pLSA-ISM on three datasets used.

3.3.2 Localisation

To compare the performance between ABS-pLSA, TSI-pLSA and pLSA-ISM, we evaluated them using unsegmented KTH dataset (with unknown centroid location) and tested whether they could localise the occurrence of a motion and recognise the motion. We also exploited the human motion data used by Blank et al. [1] for giving some qualitative results (Their data shares only 3 motion classes with KTH and there are only 10 sequences per class which is not sufficient for a quantitative test).

Quantitative test was done on unsegmented KTH dataset using the classifiers learnt in the previous experiment. Table 5 summarises the results obtained from ABS-pLSA, TSI-pLSA and pLSA-ISM. Some qualitative test results on both unsegmented KTH data and sequences from Blank et al. are shown in Figure 5.

	ABS-pLSA	TSI-pLSA	pLSA-ISM
KTH DB:			
- Accuracy(%)	41.55	61.27	71.83
- Testing time (s)	9.64	9.81	9.78

Table 5. Comparison between recognition results obtained from ABS-pLSA, TSI-pLSA and pLSA-ISM.

We can observe from this experiment that our pLSA-ISM works better than the other two pLSA algorithms. The reason may be our method provides a stronger prior on centroid locations whose association with the semantic of

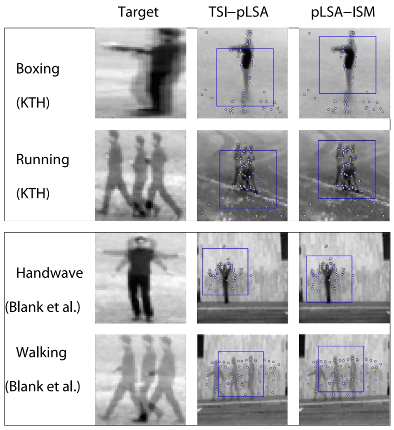

Figure 5. Localisation result on KTH dataset and sequences from Blank et al. using TSI-pLSA and pLSA-ISM.

cuboids has been learnt while TSI-pLSA assumes uniform distribution of centroid locations.

3.3.3 Retraining

We conducted this experiment to evaluate the performance of our retraining algorithm. KTH dataset was exploited in this experiment. The setting for training pLSA-ISM was the same as the one shown in Table 3, and we used leave-one-out cross validation (testing on segmented KTH data). Different from the first experiment, we varied the number of samples for training (we will use 'number of subjects' to describe the amount of data later and there are around 24 samples associated with each subject). In control set-up, we provided centroid locations (i.e. using segmented KTH data) for batch training. In test set-up, we used unsegmented KTH data for incremental training (i.e. retrain an initial model with a certain amount of new unsegmented data).

Firstly, the control set-up was used to determine the minimum amount of data to obtain a pLSA-ISM model with an acceptable performance (e.g. over 70% accuracy), and eventually 5 subjects was used to obtain an initial model. Then in the test set-up, we re-trained the initial model with various amount of data. The result is shown in Table 6.

	Total number of subjects used (prop. to sample size)					
	1	5	10	15	20	24
Control set-up	67.46	73.80	77.50	80.37	81.67	83.92
Test set-up	N/A	N/A	77.32	78.03	77.32	82.07

Table 6. The accuracy (%) obtained by pLSA-ISM through retraining is shown. Control set-up involves batch training using segmented KTH data (24 samples associated with 1 subject) while test set-up involves retraining of an initial model (built from 5 subjects) using unsegmented samples. Note that if the number of subject is shown as 10, this means a batch of 10×24 samples was used in training in the control set-up while there was a batch of 5×24 samples was added to retrain the initial model in the test set-up.

The result shows that pLSA-ISM can be retrained by unsegmented data to achieve a similar accuracy as if segmented data was used. Besides, pLSA-ISM needs only 5 subjects (120 samples) to achieve accuracy over 70% while WX-SVM needed more than 15 subjects to achieve the same accuracy according to our experience. This indicates another advantage of our unsupervised model over SVM.

4. Conclusion

This paper introduces a novel generative part-based model which extends pLSA to capture both semantic (content of parts) and structural (connection between parts) information for learning motion categories. Experimental results show that our model can improve recognition accuracy by using structural cues and it performs better in motion localisation than other pLSA models supporting structural information. Although our model usually requires a set of training samples with known centroid locations, a retraining algorithm is introduced to accept samples with unknown centroids so that we can reduce the amount of human intervention in model reinforcement.

Acknowledgements. SW is funded by the Croucher Foundation and TK is supported by the Toshiba and the Chevening Scholarship.

References

[1] M. Blank, L. Gorelick, E. Shechtman, M. Irani, and R. Basri. Actions as space-time shapes. In *Proc. ICCV*, pages 1395–1402, 2005.

[2] O. Boiman and M. Irani. Detecting irregularities in images and in video. In *Proc. ICCV*, pages 462–469, 2005.

[3] P. Dollár, V. Rabaud, G. Cottrell, and S. Belongie. Behavior recognition via sparse spatio-temporal features. In *ICCV Workshop: VS-PETS*, 2005.

[4] A. A. Efros, A. C. Berg, G. Mori, and J. Malik. Recognizing action at a distance. In *Proc. ICCV*, pages 726–733, 2003.

[5] C. Fanti, L. Zelnik-Manor, and P. Perona. Hybrid models for human motion recognition. In *Proc. CVPR*, pages 1166–1173, 2005.

[6] R. Fergus, L. Fei-Fei, P. Perona, and A. Zisserman. Learning object categories from google's image search. In *Proc. ICCV*, 2005.

[7] T. Hofmann. Unsupervised learning by probabilistic latent semantic analysis. *Machine Learning*, 42(1-2):177–196, 2001.

[8] Y. Ke, R. Sukthankar, and M. Hebert. Efficient visual event detection using volumetric features. In *Proc. ICCV*, pages 166–173, 2005.

[9] I. Laptev. On space-time interest points. *IJCV*, 64(2-3):107–123, 2005.

[10] B. Leibe, E. Seemann, and B. Schiele. Pedestrian detection in crowded scenes. In *Proc. CVPR*, pages 878–885, 2005.

[11] J. C. Niebles, H. Wang, and L. Fei-Fei. Unsupervised learning of human action categories using spatial-temporal words. In *Proc. BMVC*, 2006.

[12] C. Schuldt, I. Laptev, and B. Caputo. Recognizing human actions: A local svm approach. In *Proc. ICPR*, 2004.

[13] E. Shechtman and M. Irani. Space-time behavior based correlation. In *Proc. CVPR*, pages 405–412, 2005.

[14] J. Sivic, B. Russell, A. A. Efros, A. Zisserman, and B. Freeman. Discovering objects and their location in images. In *Proc. ICCV*, 2005.

[15] Y. Song, L. Goncalves, and P. Perona. Unsupervised learning of human motion. *PAMI*, 25:814–827, 2003.

[16] A. Yilmaz and M. Shah. Recognizing human actions in videos acquired by uncalibrated moving cameras. In *Proc. ICCV*, 2005.